Analytica Chimica Acta 1039 (2018) 108–115

Contents lists available at ScienceDirect

Analytica Chimica Acta

journal homepage: www.elsevier.com/locate/aca

Lectin-mediated in situ rolling circle amplification on exosomes for probing cancer-related glycan pattern

Yimei Feng, Yuna Guo, Yiran Li, Jing Tao, Lin Ding*, Jie Wu**, Huangxian Ju

State Key Laboratory of Analytical Chemistry for Life Science, School of Chemistry and Chemical Engineering, Nanjing University, Nanjing, 210023, PR China

HIGHLIGHTS

- An exosomal array-based strategy for multiplexed detection of cancer-related glycans on exosomes has been established.
- The exosomal glycan information is directly extracted and amplified by in situ rolling circle assembly of DNA probes..
- The strategy obviates the requirement for pre-labeling of exosomes.
- The strategy has been used for comparing glycan pattern between exosomes as well as between exosomes and cells.
- The strategy can be also used for in situ monitoring exosomal glycan remodeling processes

GRAPHICAL ABSTRACT

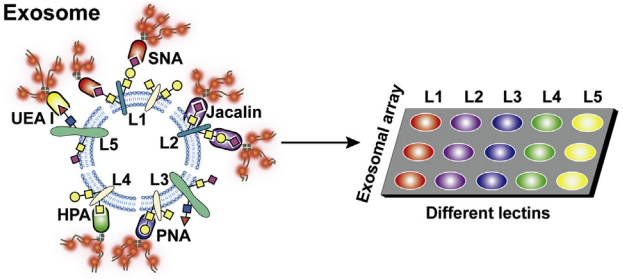

ARTICLE INFO

Article history:
Received 5 May 2018
Received in revised form
9 July 2018
Accepted 17 July 2018
Available online 19 July 2018

Keywords:
Glycan
Exosome
Array
Lectin
In situ
Rolling circle amplification

ABSTRACT

Exosomal surface glycans play important roles in microvesicle protein sorting and exosome-cell interactions, and also provide promising biomarkers for various diseases. However, in situ detection techniques for exosomal glycans are largely lacking. In this work, an exosomal array is fabricated for probing cancer-related exosomal glycan signatures by lectin recognition-mediated in situ rolling circle assembly of fluorophore-labeled DNA. Different from commonly used lectin array, the proposed strategy enables the direct and amplified conversion of glycan recognition signals to fluorescence detection signals. Focusing on tumor-associated glycans including sialic acids, fucose and truncated *O*-glycans, the method has been used not only to compare glycan patterns between exosomes with different origins, but also to reveal the specific exosomal glycan characteristics compared to their parent cells. The limits of detection were identified to be 5.4×10^6 and 1.3×10^6 particles mL^{-1} for HeLa and PANC-1 exosomes, respectively. The dynamic ranges were 4.7×10^5 to 4.7×10^8, 4.7×10^8 to 4.7×10^9 for HeLa exosomes, and 4.7×10^5 to 1.2×10^9, 1.2×10^9 to 4.7×10^9 particles mL^{-1} for PANC-1 exosomes. The remodeling of exosomal glycans can also be monitored as demonstrated on the cleavage of sialic acids under sialidase treatment. It could be anticipated that this strategy would become a powerful tool for development of exosome-based glyco-biomarkers and elucidation of biological significance of exosomal glycans.

* Corresponding author.
** Corresponding author.
E-mail addresses: dinglin@nju.edu.cn (L. Ding), wujie@nju.edu.cn (J. Wu).

https://doi.org/10.1016/j.aca.2018.07.040
0003-2670/

1. Introduction

Exosomes are small membrane vesicles with an approximate size of 30–150 nm that originate from the fusion of the multivesicular endosomes with the plasma membrane [1,2]. Since exosomes can deliver plenty of functional biomolecules including nucleic acids, proteins and lipids into recipient cells [3–5], they play an important role in cell-cell information transfer, and emerge as potential targets for disease diagnosis [6,7] and carriers for therapeutic intervention [8].

Regarding the cargo molecules packaged in exosomes, only until recently have the exosomal glycans attracted research interests [9–11]. Glycans are linear or branched oligosaccharides built from ~10 types of monosaccharide building blocks. These sugar chains can be covalently attached to underlying proteins via *N* linkage to asparagine (*N*-glycans) or *O* linkage to serine/threonine (*O*-glycans). Glycosylation is one of the most common post-translational modification of proteins and lipid in eukaryotic cells [12], and regulates the development and progression of many types of diseases, such as cancer [13,14]. The glycan signature of exosomes provides a valuable handle for understanding of the complicated protein sorting mechanism involved in exosomal biogenesis [15,16], and also the recognition and targeting tendency between exosomes and recipient cells [17]. In particular, considering the close relationship between exosomes with exosome-forming cells, the glycan expression on exosomes may reflect certain glyco-features of the parent cells [18], suggesting the potential role of exosomes as glyco-biomarker carriers [19]. Although the significance of exosomal glycans has become a consensus, the development has lagged behind due to the complex structure of glycans and the lack of sensitive and facile analytical methods for exosomal surface glycans.

There are only limited literature discussing the detection methodology for exosomal glycans, which can be mainly divided into two classes. The first is mass spectrometry-based destructive methods [17,18,20]. They suffer from complicated operation procedure and are time-consuming. The second is lectin array-based strategies [16,19,21–23], in which an array of lectin-immobilized spots are fabricated for capturing exosomes labeled with fluorescent dyes. Owing to the specific recognition capability of lectins toward glycans [24], the lectin array-based methods can provide in situ glycan pattern of exosomes. However, the glycan expression extent is indirectly derived from the amount of captured exosomes, which is susceptible to influence by various factors including, for example, the lectin-glycan binding affinity. And the sensitivity and stability of these methods are impaired by problems of protein denaturation and active site inaccessibility due to the surface-confined format of lectins [25]. Other inconvenience of these methods includes the requirement for pre-labeling of exosomes and the difficulty from connection with a signal amplification module. The latter is because one needs to use another type of recognition/assembly to introduce signal amplification unit on the exosomal surface, leading to a more complicated experiment design.

With these issues in mind, we turn to fabrication of an exosomal array for facile, direct and multiplexed probing of cancer-related glycan signatures on exosomal surfaces by lectin recognition-mediated in situ rolling circle assembly of fluorophore-labeled DNA (Scheme 1). Upon incubating the exosomal array with a panel of biotinylated lectins, the distinct expression extents of multiple glycans on exosomes can be translated to the binding quantity of corresponding biotinylated lectins using lectin moiety as the recognition unit. To amplify these binding signals, the other biotin moiety acts as the mediator for docking with a rolling circle amplification (RCA)-initiating biotin-primer by means of biotin-streptavidin binding. After RCA reaction [26], multiple Cy3-labeled DNA probes (Cy3-probe) can hybridize to the tandemly linked copies generated from a single biotin-primer, thus enhancing the fluorescent detection sensitivity. This exosomal array-based design is different from common lectin-array format in two aspects: 1) lectins in solution are used to directly reflect the glycan abundance; 2) the lectin-glycan recognition signals can be conveniently amplified by in situ RCA on exosomes. Using the proposed method, glycan pattern comparison between exosomes from different cancer cells (cervical cancer cell HeLa and pancreatic cancer cell PANC-1) and between exosomes and parent cells has been achieved, and the changes from exosomal glycan remodeling have been in situ monitored.

2. Experimental

2.1. Materials and reagents

α2-3,6,8,9 Neuraminidase A (sialidase), T4 DNA ligase, Phi29 DNA polymerase, exonuclease I (Exo I), exonuclease III (Exo III) and dNTPs were obtained from New England Biolabs, Inc. (USA). The biotinylated lectins, including biotinylated *Sambucus Nigra* agglutinin (biotin-SNA), biotinylated *Artocarpus intergrifolia* agglutinin (biotin-Jacalin), biotinylated peanut agglutinin (biotin-PNA) and biotinylated *Ulex europaeus* agglutinin I (biotin-UEA I) were purchased from Vector Laboratories (USA). The specificities of these lectins are shown in Table S1. Biotinylated *Helix pomatia* agglutinin (biotin-HPA), bovine serum albumin (BSA), streptavidin, Cy3-streptavidin and 4-(2-hydroxyethyl)-1-piperazineethanesulfonic acid (HEPES) were purchased from Sigma-Aldrich Inc. (USA). The anti-CD63 antibody, anti-CD9 antibody and horseradish peroxidase (HRP) conjugated goat anti-rabbit IgG were purchased from Abcam Trading Co., Ltd. (USA). The Accu West ECL Blaster Western blotting HRP substrate was purchased from Bioelite Co. Ltd. (Nanjing, China). The aldehyde-modified glass slides were purchased from Shanghai Baio Technology Co. Ltd (China). The aldehyde/sulfate latex beads (4% w/v, 3.9 μm) were from Invitrogen™ Thermo Fisher Scientific (USA). Phosphate buffer saline (0.01 M, containing 135 mM NaCl, 2.7 mM KCl, 1.5 mM KH_2PO_4 and 8 mM K_2HPO_4, pH = 7.2–7.4) was purchased from KeyGEN Biotech Co. Ltd. (China). Cell lysis buffer, SDS-polyacrylamide gel electrophoresis (SDS-PAGE) buffer, Western blotting blocking buffer, antibody dilution buffer, secondary antibody dilution buffer, and all HPLC-purified oligonucleotides used in this work were purchased from Sangon Biotechnology Co. Ltd. (China). The detailed sequences of all oligonucleotides were listed in Table S2. The aqueous solutions used in this work were prepared using ultrapure water (≥18 MΩ, Milli-Q, Millipore).

2.2. Apparatus

The glycan array was scanned with a Biochip Analysis System (Capitalbio, China). For exosomal isolation, a Beckman Coulter OPTIMA L-100XP ultracentrifuge (70 Ti Rotor) was used. Flow cytometric analysis was performed on a Cytomics FC500 flow cytometer (Beckman Coulter, USA). The exosomal morphology was observed with a JEOL JEM-2100 transmission electron microscopy (TEM, Japan). Agarose gel electrophoresis was performed in a DYCP-31DN agarose electrophoresis cell (Beijing Liuyi Biological Technology Co., Ltd.), and SDS-PAGE was performed at a Mini-PROTEAN Tetra cell (Bio-Rad, USA), both of which were visualized using a Bio-Rad ChemiDoc XRS system (Bio-Rad, USA). The cell numbers were determined by a Countess® II Automatic cell counter (Thermo Fisher Scientific, USA).

2.3. Cell culture and treatment

A cervical cancer cell line HeLa and a pancreatic cancer cell line

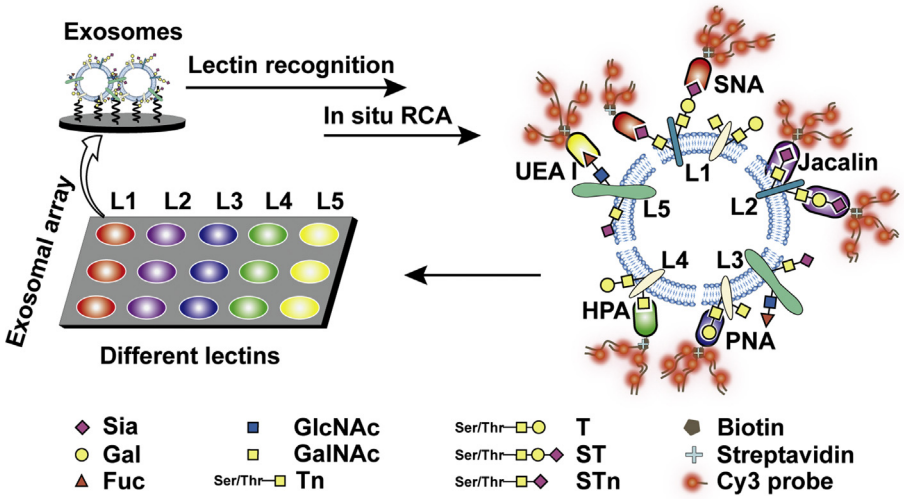

Scheme 1. Schematic illustration of lectin-mediated in situ rolling circle amplification (RCA) on an exosomal array for detection of cancer-related exosomal glycan pattern. Sia, 5-N-acetylneuraminic acid; Gal, galactose; Fuc, fucose; GlcNAc, *N*-acetylglucosamine; GalNAc, *N*-acetylgalactosamine; Tn, Tn antigen; T, T antigen; ST, sialylated T antigen; STn, sialylated Tn antigen. Five types of biotinylated lectins are used: SNA, *Sambucus Nigra* agglutinin; Jacalin, *Artocarpus intergrifolia* agglutinin; PNA, peanut agglutinin; HPA, *Helix pomatia* agglutinin; UEA I, *Ulex europaeus* agglutinin I.

PANC-1 were purchased from KeyGEN Biotech Co., Ltd. (Nanjing, China). The two types of cells were cultured in high-glucose Dulbecco's modified Eagle's medium (DMEM) supplemented with 10% fetal bovine serum (FBS, Gibco, Thermo Fisher Scientific, USA), penicillin (80 U mL^{-1}) and streptomycin (80 μg mL^{-1}) at 37 °C in a humidified atmosphere containing 5% CO_2, respectively.

For preparation of cell lysates, well-washed PANC-1 and HeLa cells were respectively mixed with the lysis buffer which contained 1 mL of radioimmunoprecipitation assay (RIPA) buffer, 1 μL of 1 M phenylmethylsulfonyl fluoride (PMSF) and 1 μL of 1 M protease inhibitor. After incubation for 30 min at 4 °C under gentle shaking, the mixture was centrifuged at 16000 g for 20 min at 4 °C and the supernatant was collected. The protein concentration was determined by a bicinchoninic acid (BCA) assay.

2.4. Isolation of exosomes

Exosomes were collected by sequential centrifugation from the supernatant media of PANC-1 and HeLa cells, respectively, following the published literature protocol [5,16]. In brief, upon reaching 50% confluence, the cells were washed three times with PBS to remove the FBS and then cultured in FBS-free DMEM for 24 h. The supernatant media were then collected, and subjected to centrifugation at 300g for 10 min, 2000 g for 10 min and 10000 g for 30 min at 4 °C to remove dead cells, large cellular debris and contamination microvesicles, respectively [27]. After filtration through a 0.22 μm filter, exosomes were collected by centrifugation at 120,000 g for 70 min at 4 °C, followed by washing with PBS and re-ultracentrifugation. The exosomes obtained were then resuspended in PBS and stored at −80 °C for further use. The morphology of exosomes was observed using TEM after negative staining, and the size distribution and concentration of exosomes were determined by Nanoparticle Tracking Analysis (NTA, NanoSight, UK). The protein concentration of exosomes was analyzed by BCA.

2.5. Western blotting

The exosome and cell lysate samples of the same protein concentration were respectively mixed with 1x loading buffer and separated by SDS-PAGE, followed by being transferred to a nitrocellulose (NC) membrane. After blocking and washing, the NC membrane was blotted with anti-CD63 antibody (1:2000 dilution) and anti-CD9 antibody (1:2000 dilution) overnight, respectively, followed by incubation with HRP-conjugated secondary antibody for 2 h. The membrane was then incubated with ECL Blaster Western blotting HRP substrate and the bands were visualized by the Bio-Rad ChemiDoc XRS system.

2.6. Preparation of exosomal array

A predesigned and laser etched hydrophobic frame with 36 holes (3 mm diameter, 12 rows × 3 columns with edge-to-edge separation of 2 mm) was fitted to an aldehyde-modified glass slide, and 4 μL of exosomal solution was dropped on each spot and incubated for 2 h at 4 °C. The slide was then thoroughly washed with washing buffer (PBS containing 0.05% Tween 20), and the unreacted aldehyde groups were blocked with the blocking buffer (PBS with 1 M glycine and 20% BSA) for 1 h at 37 °C [28,29]. After washing with the washing buffer and drying with nitrogen stream, the exosomal array was obtained for further use.

2.7. In situ RCA-based detection of glycans on exosomal array

For preparation of RCA circular template, 12 μL of padlock probe (50 μM) and 24 μL of ligation probe (50 μM) were first annealed under 95 °C for 15 min, respectively, which were then mixed in 196 μL of T4 DNA ligase reaction buffer (50 mM Tris-HCl containing 10 mM $MgCl_2$, 1 mM ATP and 10 mM DTT). After addition of 8 μL of T4 DNA ligase (400 U μL^{-1}), the mixture was incubated overnight at 16 °C followed by inactivation of T4 DNA ligase with 65 °C heating for 15 min. Then the exonucleases Exo I (8 μL, 20 U μL^{-1}) and Exo III (8 μL, 100 U μL^{-1}) were added to eliminate the ssDNA and dsDNA by incubation for 1 h at 37 °C. The final circular template was precipitated with ethanol and stored at 4 °C for further use.

For RCA-based detection of glycans on the exosomal array (1.9×10^7 exosomes per spot), 4 μL of biotinylated lectins in 10 mM HEPES at respective optimal concentrations were spotted on the exosomal array with 3 spots per biotinylated lectin and incubated at 4 °C for 1 h. In this work, 5 types of biotinylated lectins with

distinct specificities were used (Table S1), and the metal ions required for lectin binding were added to lectin solutions for biotin-PNA (Ca^{2+}, Mg^{2+} of 1 mM) and biotin-UEA I (Ca^{2+}, Mn^{2+} and Zn^{2+} of 0.1 mM). Then 4 μL of streptavidin (10 μg mL^{-1}) was dropped on each spot and incubated for 30 min. After incubation with 4 μL of the biotin-primer (1 nM) at 37 °C for 30 min, the slide was subjected to incubation with the RCA reaction mixture at 37 °C for 1 h, which contained 4 μL of Phi29 DNA polymerase (10 U μL^{-1}), 0.5 μL of circular template (2.1 μM), 3 μL of dNTPs (10 mM each), 8 μL of BSA (10 mg mL^{-1}) and 19 μL of Phi29 DNA polymerase buffer (50 mM Tris-HCl, 10 mM $MgCl_2$, 10 mM $(NH_4)_2SO_4$, 4 mM DTT). After washing and drying steps, 4 μL of Cy3-probe (100 nM) was added to each spot for hybridization at 37 °C for 30 min, followed by 3-time washing. The fluorescence intensity (FI) of the array was measured on the Biochip Analysis System with parameters set as PMT 550 and Power 95. The original fluorescent signals are black and white, which were converted to pseudocolor images based on the intensity (see the color scale bar) using GenePix Pro 7 software. The standard deviation was obtained from 3 replicate data points. The proposed method was also used to analyze the glycan expression pattern on cell surface by replacing exosomes with cells for covalent immobilization on aldehyde-modified glass slides.

For detection of exosomal glycans without RCA, after incubation of the exosomal array with biotinylated lectins, 4 μL of Cy3-streptavidin (10 μg mL^{-1}) was dropped on each spot, and incubated at 37 °C for 30 min. The slide was then washed with the washing buffer thrice and dried with nitrogen stream. The fluorescence signals were measured as described above.

2.8. Sialidase treatment of exosomal array

After dropping 4 μL of sialidase (0.5 U μL^{-1}) on each spot of the as-prepared exosomal array (1.9×10^7 exosomes per spot), the slide was blocked with the blocking buffer and then allowed to incubate with biotinylated lectins. The following steps were the same as described above. The FI values were expressed as a mean ± SD of replicate spots (n = 3). The variation upon sialidase treatment was analyzed by one-way ANOVA.

3. Results and discussion

3.1. Isolation and characterization of exosomes

The HeLa and PANC-1 exosomes were respectively isolated from cell culture media using differential centrifugation protocol [5,16]. A prototypical cup shape [16] was observed for the majority of both types of exosomes by transmission electron microscopy (Fig. 1a and b). The nanoparticle tracking analysis showed a mean diameter of 122 nm for HeLa exosomes and 99 nm for PANC-1 exosomes (Fig. 1c). The presence of exosomal surface markers, CD63 and CD9, as verified by western blot (Fig. 1d) confirmed the identity of the exosomes. The different molecular weights for CD63 bands may result from different glycoforms of the protein [16].

3.2. Exosomal array fabrication and detection principle

In line with our goal to compare glycan expression extents on different cancer cell-derived exosomes, aldehyde-modified glass slide was chosen for indiscriminate immobilization of exosomes through a covalent linkage between the aldehyde group and the amino group of exosomal proteins. To achieve simultaneous detection of multiple cancer-related glycans on immobilized exosomes, five types of lectins with distinct binding specificities were chosen to act as the recognition moieties (Scheme 1, Table S1). We pay particular attention to two classes of most-widely occurring tumor-associated glycans [13]. The first is the terminal glycan motifs (monosaccharides that terminate the sugar chains) sialic acid (Sia), recognized by SNA, and fucose (Fuc), recognized by UEA I. The two terminal monosaccharides undergo significant changes during neoplastic progression and are closely related to poor prognosis [14]. The other is the truncated *O*-glycans (shortened *O*-glycans due to deficiency in *O*-glycan extension mechanisms [13]), including the disaccharide Galβ1-3GalNAcα-Thr/Ser (T antigen), recognized by PNA, and the monosaccharide GalNAcα-Thr/Ser (Tn antigen), recognized by HPA, and their sialylated forms, ST and STn. They are important diagnosis and prognostic markers and targets for anticancer vaccines [13]. Jacalin that can bind the above-mentioned four types of *O*-glycans was also used in this work. The glycan expression pattern on exosomal surfaces was investigated using the chosen panel of lectins that were conjugated with biotin. The biotin handle enabled the introduction of a RCA-based signal amplification module through sequential incubation with streptavidin, biotin-primer, RCA reaction mixture and finally Cy3-probe. As seen from Fig. 2a, the RCA reaction endowed an amplification ratio of 15.6 obtained by comparing the RCA-based FI (column B) with the FI from spots without RCA (using Cy3-streptavidin to replace streptavidin to bind biotin-SNA, column A), indicating that the primer-initiated RCA generated a long DNA strand for hybridizing multiple Cy3-probes for signal enhancement. The dependence of RCA reaction on the streptavidin, biotin-primer and RCA reaction mixture were respectively verified by the significantly decreased FI from spots for streptavidin-free (column E), biotin-primer-free (column F) and RCA reaction mixture-free (column G) cases with other steps unchanged. The detection specificity could be demonstrated by investigation of the signals when exosomes or biotin-lectins were not engaged. In the absence of either HeLa exosome (column C) or biotin-SNA (column D), only background-level signals were observed, suggesting the specific binding between the biotinylated lectin and exosomes.

The feasibility of using the designed sequences to perform RCA reaction was verified by agarose gel electrophoresis experiments. As shown in Fig. 2b, the bands for padlock probe (lane 2) and circular template (lane 3) were at the same location, which could be explained by the same strand length. In the case of preparing circular template without T4 DNA ligase added, no band could be observed (lane 4), due to the cleavage of the padlock and ligation probes by Exo I and Exo III. This suggested the essential role of T4 DNA ligase for preparation of the circular template. The one-pot incubation of the primer and RCA reaction mixture yielded a new set of trailing bands which moved much slower (lane 5), demonstrating the generation of concatemer ssDNA with different length [30].

3.3. Detection performance

Before evaluation of the detection performance of the proposed method, concentrations of the biotinylated lectins (Fig. S1) and RCA reaction time (Fig. S2) were optimized. Given the variation of binding affinity among different lectin-glycan recognition pairs, the concentration of each type of biotinylated lectins was individually optimized. To obtain the relationship between FI and the exosomal concentration, exosomal suspensions of different concentrations from 4.7×10^5 to 4.7×10^9 particles mL^{-1} were spotted on the aldehyde-modified glass slide. The fluorescent scanning images for two types of exosomes were shown in Fig. 3. For both types of exosomes, the FI showed an initial slow increase and later fast increase behavior depending on exosomal concentration, with inflection points observed at 4.7×10^8 and 1.2×10^9 particles mL^{-1} for HeLa and PANC-1 exosomes, respectively. The greater signals

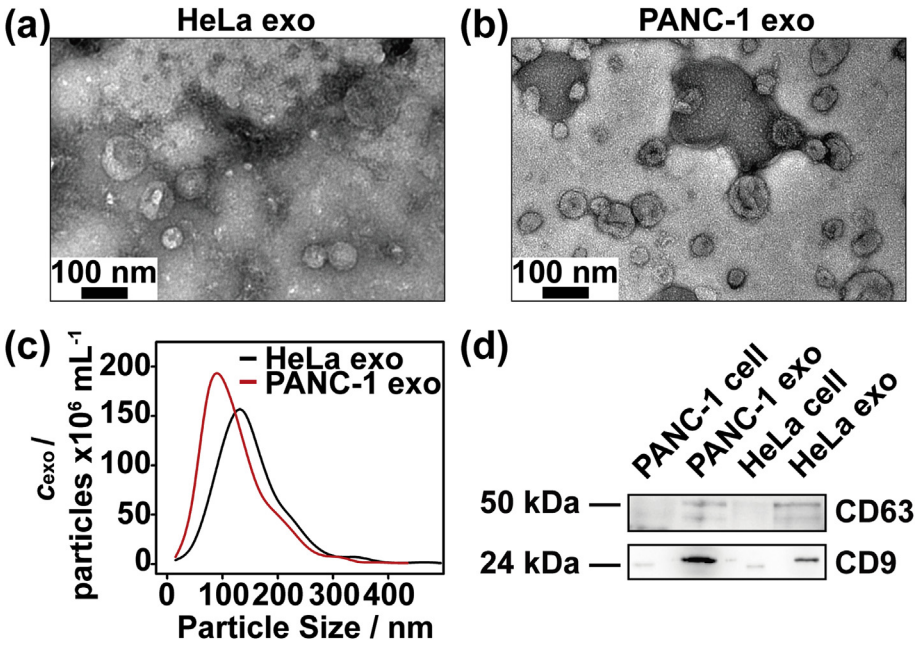

Fig. 1. Characterization of isolated exosomes (exo). TEM images of HeLa (a) and PANC-1 (b) exosomes. (c) Exosomal concentrations and size distribution analyzed by NTA. (d) Western blot analysis of PANC-1 and HeLa cell lysates and exosomes using anti-CD63 and anti-CD9 antibodies.

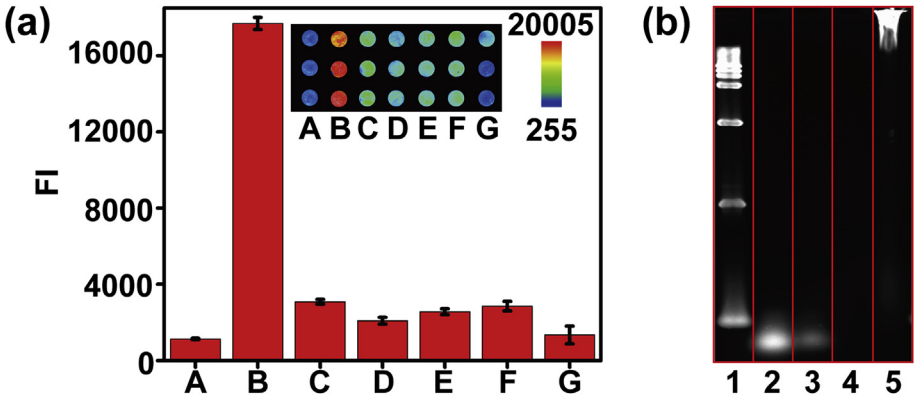

Fig. 2. Validation of experimental feasibility. (a) FI of biotin-SNA incubated HeLa exosomal spots after Cy3-streptavidin incubation (A) or sequential incubation with streptavidin, biotin-primer, RCA reaction mixture and Cy3-probe (B). (C) to (G): FI obtained by an otherwise identical procedure used for the acquisition of FI in (B) except in the respective absence of exosome (C), biotin-SNA (D), streptavidin (E), biotin-primer (F), and RCA reaction mixture (G). Inset of (a) is the corresponding fluorescent image with the color scale bar indicating the FI. (b) Agarose gel electrophoresis characterization of RCA-related processes. Lane 1, DNA marker; lane 2, padlock probe; lane 3, products of circular template preparation process; lane 4, products of circular template preparation process without T4 DNA ligase added; lane 5, products of RCA reaction.

obtained on HeLa exosomes indicated a higher expression of terminal Sia on HeLa exosomal surfaces. To characterize the detection sensitivity, detectable concentration was defined as the exosomal concentration that exhibited statistically significant difference ($p < 0.05$) of FI compared with that for concentration of 0 particles mL^{-1}, which was 4.7×10^6 particles mL^{-1} for both HeLa and PANC-1 exosomes, calculated by one-way ANOVA [31]. The limit of detection (LOD), defined as the concentration that corresponded to 3 standard deviations above the control (0 particles mL^{-1}), was also obtained as 5.4×10^6 and 1.3×10^6 particles mL^{-1} for HeLa and PANC-1 exosomes, respectively. The exosomal detection sensitivity of the proposed method was higher than that obtained by size exclusion chromatography (2.9×10^7 particles mL^{-1}) [32] and surface-enhance Raman spectroscopy (10^9 particles mL^{-1}) [33], which could be attributed to the efficient amplification of lectin recognition signals by the biotin-initiated RCA.

3.4. Cancer-related glycan patterns on exosomes and their parent cells

The high sensitivity and multiplexed analysis capability allowed the proposed method to be used for profiling exosomal glycan patterns using HeLa and PANC-1 exosomes as the models. Both types of exosomes exhibited strongest binding to biotin-SNA, moderate binding to biotin-Jacalin and relatively low binding to the other three types of biotinylated lectins (Fig. 4a and c). This binding pattern was also verified by flow cytometric analysis using aldehyde-based latex beads for capturing nanoscale exosomes, due to the weak light scattering of single exosome [31] (Fig. S3). Compared with the exosomal array-based method, flow cytometry-based method allows limited multiplexing of glycans in each test. Moreover, it suffers from the issue of crosslinking of exosome-immobilized beads by lectins bearing several subunits. This might

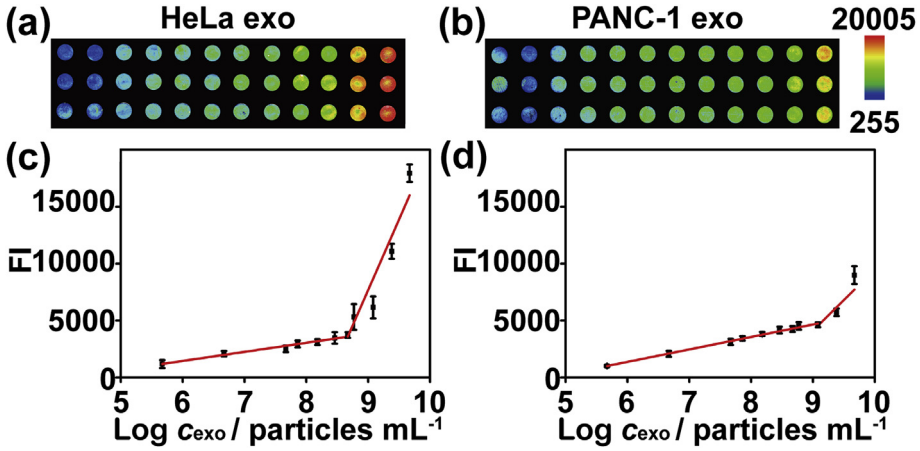

Fig. 3. Fluorescent images of HeLa (a) and PANC-1 (b) exosomal arrays fabricated with different exosomal concentrations and bound by biotin-SNA, and the dependence of FI on the logarithm of HeLa (c) and PANC-1 (d) exosomal concentrations. From left to right in (a) and (b), the exosomal concentrations are 0, 4.7×10^5, 4.7×10^6, 4.7×10^7, 7.3×10^7, 1.5×10^8, 2.9×10^8, 4.7×10^8, 5.9×10^8, 1.2×10^9, 2.4×10^9, 4.7×10^9 particles mL^{-1}.

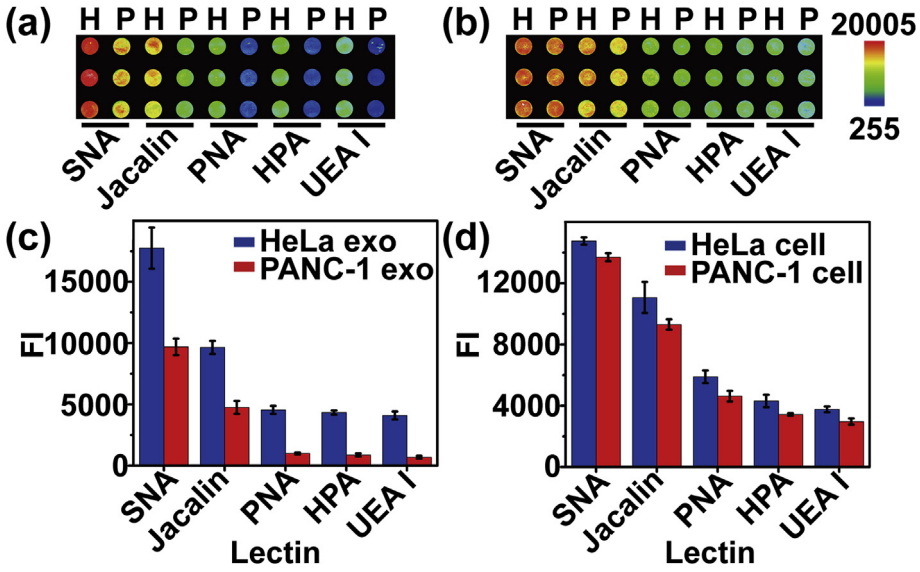

Fig. 4. Comparison of glycan patterns between different exosomes as well as between exosomes and their parent cells. Fluorescent images of the exosomal (a) and cellular (b) arrays with labels H and P representing HeLa and PANC-1 respectively. (c) and (d) are the corresponding histograms for (a) and (b), respectively.

lead to a broader distribution of fluorescent intensities as well as non-smooth curves. The observed binding pattern suggested a pronounced expression of Siaα2-6Gal/GalNAc and the presence of truncated *O*-glycans, including sialylated and asialylated forms of T and Tn antigens, on exosomes. Although HeLa exosomes apparently displayed stronger lectin binding intensities for all types of lectins compared with PANC-1 exosomes, similar glycan profiles could be easily observed for HeLa and PANC-1 exosomes. This phenomenon was in concordance with a previous literature reporting similar glycan signatures of exosomes derived from T-cells, melanoma and colon cancer cells [16]. Our results from cervical and pancreatic carcinoma cell derived exosomes provided more evidence supporting this conclusion, and also demonstrated the capability of using the proposed method to interrogate the exosomal glycans.

In addition to comparing exosomal glycans with different origins, the glycan patterns of exosomes and their parent cells were also compared. The cell surface glycan patterns were profiled by replacing exosomes with cells for fabrication of the arrays (Fig. 4b and d). Compared with parent cells, exosomes exhibited higher ratios of FI from SNA to FI from truncated *O*-glycan specific lectins (Jacalin, PNA, HPA). This might be explained by the enrichment of sialoglycoproteins on exosomal surface [4,7,9,16]. Considering the cancer-indicative role of cell surface Sia, sialylated glycans on exosomes might serve as potential biomarkers for point-of-care diagnosis with much easier accessibility. In addition, the hardly detectable FI from UEA-1 on PANC-1 exosomes suggested a depletion of O blood group glycoconjuates [7,16]. These results indicated that the exosomes carried specific glycan signatures compared with the parent cell membranes [7]. And the developed strategy also provided a valuable tool for developing glycan-associated exosomal biomarkers.

3.5. *In situ monitoring of the exosomal glycan remodeling*

The proposed method was further used for monitoring the dynamic alteration of glycan pattern on PANC-1 exosomal surface under glycosidase treatment, using sialidase (α2-3,6,8,9 neuraminidase A) as the model. After treatment, the FI from biotin-SNA

binding decreased significantly which could be attributed to the cleavage of α-2,6 linkage of terminal Sia (Fig. 5). While the signals from biotinylated Jacalin, PNA and HPA, which can bind asialylated T and Tn antigens, elevated obviously, because the cleavage of terminal Sia led to the exposure and easier accessibility of Gal/GalNAc motifs on *O*-glycans [13]. The FI from UEA I binding displayed indiscernible variation as expected. These results not only verified the detection specificity, but also demonstrated the practicality of the proposed method as a platform for in situ monitoring the glycan remodeling processes on exosomal surfaces due to the facile operation capability on surface-immobilized exosomes. The exosomal glycan remodeling may hold great promise as an alternative way to regulate the exosomal targeting tendency toward recipient cells/tissues when using exosomes as drug delivery carriers.

4. Conclusions

An exosome array was fabricated for facile, sensitive and multiplexed detection of exosomal glycan pattern. The expression extents of several types of tumor-associated glycan motifs were profiled on HeLa and PANC-1 exosomes by lectin recognition-mediated in situ rolling circle assembly of fluorophore-labeled DNA. The exosomal glycan patterns shared common features despite originating from different cell lines, and moreover, they displayed distinct ratios among glycan motifs compared with their parent cells. Owing to the convenience of glycan remodeling on surface-confined exosomes, the changes of exosomal glycans were monitored using the proposed method. By combining the large-scale microarray technique, this strategy could be applied for high-throughput profiling of exosomal glycome, thus contributing to the development of exosome-derived glycan-based biomarkers and drug targets with much easier accessibility compared with cell surface glycans. This work could also be useful in the future study of glycan-mediated exosome-involved biological processes.

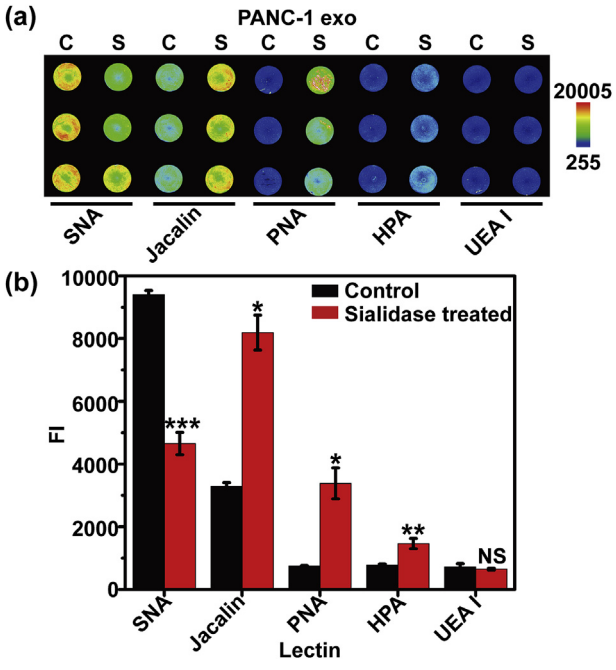

Fig. 5. Fluorescent image (a) and histogram (b) of the PANC-1 exosomal array. Labels C and S indicate spots without and with sialidase treatment, respectively, prior to incubation with biotinylated lectins. Statistically significant differences are specified by their *p*-values: $^{*}p < 0.005$; $^{**}p < 0.0005$; $^{***}p < 0.00005$, calculated by one-way ANOVA.

Conflicts of interest

There are no conflicts of interest to declare.

Acknowledgments

We gratefully acknowledge support from the National Natural Science Foundation of China (21675082, 21635005, 21575063), the National Basic Research Program of China (2014CB744501), and State Key Laboratory of Analytical Chemistry for Life Science (5431ZZXM1708).

Appendix A. Supplementary data

Supplementary data related to this article can be found at https://doi.org/10.1016/j.aca.2018.07.040.

References

[1] H. Valadi, K. Ekstrom, A. Bossios, M. Sjostrand, J.J. Lee, J.O. Lotvall, Exosome-mediated transfer of mRNAs and microRNAs is a novel mechanism of genetic exchange between cells, Nat. Cell Biol. 9 (2007) 654–659.
[2] M. Tkach, C. Théry, Communication by extracellular vesicles: where we are and where we need to go, Cell 164 (2016) 1226–1232.
[3] L. Alvarez-Erviti, Y. Seow, H. Yin, C. Betts, S. Lakhal, M.J.A. Wood, Delivery of siRNA to the mouse brain by systemic injection of targeted exosomes, Nat. Biotechnol. 29 (2011) 341–345.
[4] C. Escrevente, N. Grammel, S. Kandzia, J. Zeiser, E.M. Tranfield, H.S. Conradt, J. Costa, Sialoglycoproteins and N-glycans from secreted exosomes of ovarian carcinoma cells, PLoS One 8 (2013) e78631.
[5] Y. Liang, W.S. Eng, D.R. Colquhoun, R.R. Dinglasan, D.R. Graham, L.K. Mahal, Complex N-linked glycans serve as a determinant for exosome/microvesicle cargo recruitment, J. Biol. Chem. 289 (2014) 32526–32537.
[6] R. Kalluri, The biology and function of exosomes in cancer,, J. Clin. Invest. 126 (2016) 1208–1215.
[7] J. Gomes, P. Gomes-Alves, S.B. Carvalho, C. Peixoto, P.M. Alves, P. Altevogt, J. Costa, Extracellular vesicles from ovarian carcinoma cells display specific glycosignatures, Biomolecules 5 (2015) 1741–1761.
[8] H.C. Christianson, K.J. Svensson, T.H. van Kuppevelt, J.-P. Li, M. Belting, Cancer cell exosomes depend on cell-surface heparin sulfate proteoglycans for their internalization and functional activity, Proc. Natl. Acad. Sci. U. S. A 110 (2013) 17380–17385.
[9] O. Moreno-Gonzalo, C. Villarroya-Beltri, F. Sanchez-Madrid, Post-translational modifications of exosomal proteins, Front. Immunol. 5 (2014) 383.
[10] J.Q. Gerlach, M.D. Griffin, Getting to know the extracellular vesicle glycome, Mol. Biosyst. 12 (2016) 1071–1081.
[11] J. Costa, Glycoconjugates from extracellular vesicles: structures, functions and emerging potential as cancer biomarkers, Biochim. Biophys. Acta 1868 (2017) 157–166.
[12] A. Varki, Biological roles of glycans, Glycobiology 27 (2017) 3–49.
[13] S.S. Pinho, C.A. Reis, Glycosylation in cancer: mechanisms and clinical implications, Nat. Rev. Canc. 15 (2015) 540–555.
[14] S.R. Stowell, T. Ju, R.D. Cummings, Protein glycosylation in cancer, Annu. Rev. Pathol. 10 (2015) 473–510.
[15] C. Escrevente, S. Keller, P. Altevogt, J. Costa, Interaction and uptake of exosomes by ovarian cancer cells, BMC Canc. 11 (2011) 108.
[16] B.S. Batista, W.S. Eng, K.T. Pilobello, K.D. Hendricks-Munoz, L.K. Mahal, Identification of a conserved glycan signature for microvesicles, J. Proteome Res. 10 (2011) 4624–4633.
[17] M. Saraswat, S. Joenväära, L. Musante, H. Peltoniemi, H. Holthofer, R. Renkonen, N-linked (N-) glycoproteomics of urimary exosomes, Mol. Cell. Proteomics 14 (2015) 263–276.
[18] S. Staubach, P. Schadewaldt, U. Wendel, K. Nohroudi, F.-G. Hanisch, Differential glycomics of epithelial membrane glycoproteins from urinary exovesicles reveals shifts toward complex-type N-glycosylation in classical galactosemia, J. Proteome Res. 11 (2012) 906–916.
[19] J.Q. Gerlach, A. Kruger, S. Gallogly, S.A. Hanley, M.C. Hogan, C.J. Ward, L. Joshi, M.D. Griffin, Surface glycosylation profiles of urine extracellular vesicles, PLoS One 8 (2013) e74801.
[20] J.O. Nyalwidhe, L.R. Betesh, T.W. Powers, E.E. Jones, K.Y. White, T.C. Burch, J. Brooks, M.T. Watson, R.S. Lance, D.A. Troyer, O.J. Semmes, A. Mehta, R.R. Drake, Increased bisecting n-acetylglucosamine and decreased branched chain glycans of N-linked glycoproteins in expressed prostatic secretions associated with prostate cancer progression, Proteonomics Clin. Appl. 7 (2013) 677–689.
[21] J. Echevarria, F. Royo, R. Pazos, L. Salazar, J.M. Falcon-Perez, N.C. Reichardt,

Microarray-based identification of lectins for the purification of human urinary extracellular vesicles directly from urine samples, Chembiochem 15 (2014) 1621–1626.
[22] J.Q. Gerlach, C.M. Maguire, A. Krüger, L. Joshi, A. PrinaMello, M.D. Griffn, Urinary nanovesicles captured by lectins or antibodies demonstrate variations in size and surface glycosylation profile, Nanomedicine 12 (2017) 1217–1229.
[23] A. Shimoda, Y. Tahara, S.I. Sawada, Y. Sasaki, K. Akiyoshi, Glycan profiling analysis using evanescent-field fluorescence-assisted lectin array: importance of sugar recognition for cellular uptake of exosomes from mesenchymal stem cells, Biochem. Biophys. Res. Commun. 491 (2017) 701–707.
[24] L. Krishnamoorthy, L.K. Mahal, Glycomic analysis: an array of technologies, ACS Chem. Biol. 4 (2009) 715–732.
[25] Y. Chen, L. Ding, J. Xu, W. Song, M. Yang, J. Hu, H.X. Ju, Micro-competition system for Raman quantification of multiple glycans on intact cell surface, Chem. Sci. 6 (2015) 3769–3774.
[26] P.M. Lizardi, X. Huang, Z. Zhu, P. Bray-Ward, D.C. Thomas, D.C. Ward, Mutation detection and single-molecule counting using isothermal rolling-circle amplification, Nat. Genet. 19 (1998) 225–232.
[27] R. Maroto, Y. Zhao, M. Jamaluddin, V.L. Popov, H. Wang, M. Kalubowilage, Y. Zhang, J. Luisi, H. Sun, C.T. Culbertson, S.H. Bossmann, M. Motamedi, A.R. Brasier, Effects of storage temperature on airway exosome integrity for diagnostic and functional analyses, J. Extracell. Vesicles 6 (2017), 1359478.
[28] W. Cheng, L. Ding, Y.L. Chen, F. Yan, H.X. Ju, Y.B. Yin, A facile scanometric strategy for ultrasensitive detection of protein using aptamer-initiated rolling circle amplification, Chem. Commun. 46 (2010) 6720–6722.
[29] C. Zong, J. Wu, C. Wang, H.X. Ju, F. Yan, Chemiluminescence imaging immunoassay of multiple tumor markers for cancer screening, Anal. Chem. 84 (2012) 2410–2415.
[30] Y. Guo, Y. Wang, S. Liu, J. Yu, H. Wang, Y. Wang, J. Huang, Label-free and highly sensitive electrochemical detection of *E. coli* based on rolling circle amplifications coupled peroxidase-mimicking dnazyme amplification, Biosens. Bioelectron. 75 (2016) 315–319.
[31] S. Wang, L. Zhang, S. Wan, S. Cansiz, C. Cui, Y. Liu, R. Cai, C. Hong, I.T. Teng, M. Shi, Y. Wu, Y. Dong, W. Tan, Aptasensor with expanded nucleotide using DNA nanotetrahedra for electrochemical detection of cancerous exosomes, ACS Nano 11 (2017) 3943–3949.
[32] R. Xu, A. Fitts, X. Li, J. Fernandes, R. Pochampally, J. Mao, Y.-M. Liu, Quantification of small extracellular vesicles by size exclusion chromatography with fluorescence detection, Anal. Chem. 88 (2016) 10390–10394.
[33] J. Park, M. Hwang, B. Choi, H. Jeong, J.-h. Jung, H.K. Kim, S. Hong, J.-h. Park, Y. Choi, Exosome classification by pattern analysis of surface-enhanced Raman spectroscopy data for lung cancer diagnosis, Anal. Chem. 89 (2017) 6695–6701.